Extracting full-resolution models from seismic data to minimize systematic errors in inversion: Method and examples

Friso Brouwer, Arnaud Huck, and Nanne Hemstra, dGB Sciences
Igor Braga, Invision Geophysics

Creating an accurate subsurface model is paramount to many geophysical and geological workflows. Examples are background models for seismic inversion, rock property models for reservoir characterization, and geological models of depositional elements for seismic morphological interpretation.

The standard workflow for creating subsurface models using seismic data is stratal slicing. The stratal slicing approach, however, may break down in the case of complex stratigraphic or tectonic structuring, such as shelf-to-basin clinoforms, delta lobe switching, deep-water channel-fan complexes, and deformation due to salt tectonics.

This paper illustrates how the results obtained with high-resolution inversion and the incorporation of a stratigraphically consistent low-frequency model generated through horizon mapping—called the HorizonCube—improves the quality of the estimation of the subsurface parameters in structural complex settings. Using two data examples with different seismic data and geological settings from the North Sea and offshore Brazil, the paper will demonstrate the increased accuracy of the final inversion result using a data-driven HorizonCube.

Generalized models: An obstacle to the seismic inversion of reservoir properties

Different data and methodologies are available for model building. If only wells are available, a model might be built using manual correlation between logs, interpolation in 3D space, and optional stochastic modeling.

The availability of seismic data, however, offers significant advantages as we can now apply data control on the 3D structures described in the model. The standard workflow used for this is stratal slicing, a well established technique for building low-frequency models in model-based seismic inversions (Russell and Hampson, 1991) and a technology often used for the interpretation of seismic geomorphology (Zeng, 1998a, 1998b).

The stratal slicing workflow starts with a number of interpreted horizons. These horizons define the top and bottom of packages. Additional intermediate horizons can be modeled using relationships with bounding horizons—typically "proportional," "parallel to upper," "parallel to lower" (Figure 1). This methodology works well in settings with pseudo layer-cake deposition and gentle tectonic deformation.

While stratal slicing is a powerful workflow that is effective in a large number of situations, the stratal slicing approach may break down in the case of complex stratigraphic or tectonic structuring. Examples include shelf-to-basin clinoforms, switching delta lobe geometries, deep-water channel-fan complexes, and structuring caused by salt tectonics. In these and other cases, generalized models are no longer valid.

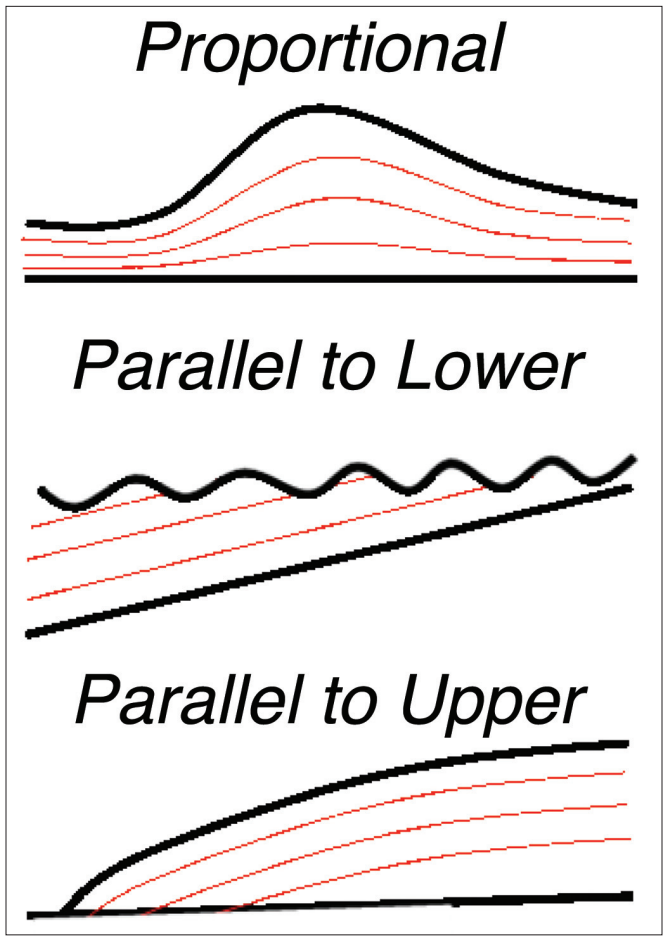

Figure 1. *Modes of traditional model building. Sparse horizons (black) are interpreted manually. Based on rules that can vary by packages, infill horizons are created for model building or interpretation purposes.*

Figure 2 compares a typical example of seismic data that is suitable for a model-based approach (Figure 2a) and a typical example of seismic data more suitable for a data-driven approach (Figure 2b).

The HorizonCube: Full-resolution horizon tracking for model building

The solution to overcome the limitations of a model-based workflow is to extract more detail from the seismic data, as all structural detail needed for seismic inversion is already registered in the seismic measurement. If we could convert that information into a usable form for model building, we could then apply the necessary detail to the models to work in areas with complex stratigraphic structures or tectonic deformation.

To achieve this amount of detail, manual tracking might

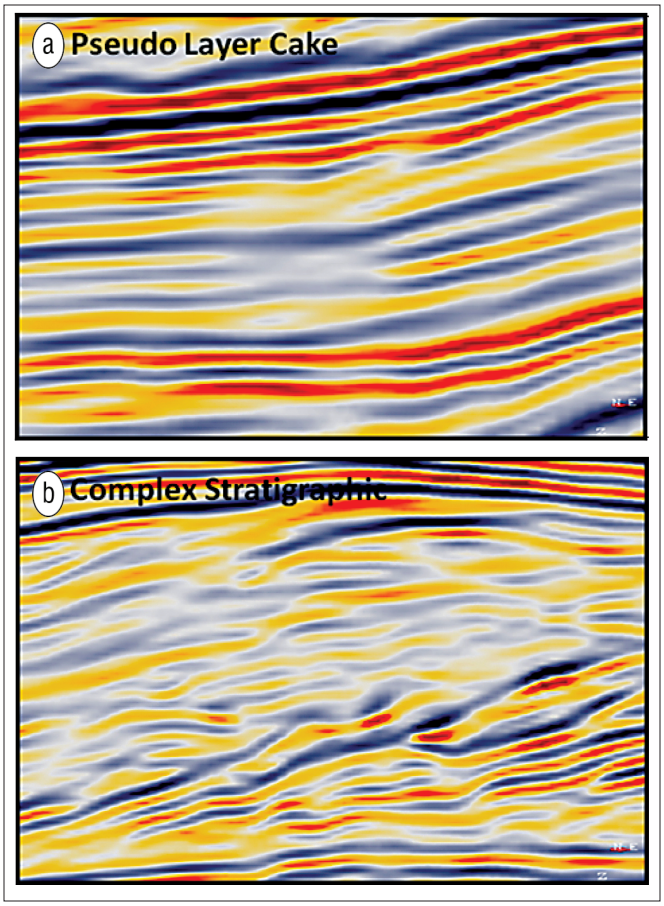

Figure 2. *(a) A pseudo layer-cake setting suitable for model-based workflows. (b) A complex stratigraphic setting in which data-driven model-building algorithms often provide better results.*

not be feasible for two reasons: tracking many horizons by itself is time consuming, and the additional horizons needed to refine a model to the necessary accuracy are often complex geologically and/or in their seismic expression, therefore taking up increasingly more interpretation time per interpreted horizon. Combined, this leads to the observation that manually increasing model accuracy escalates the amount of interpretation time needed. The challenge is thus to build a tracking algorithm that allows us to extract all detail from the seismic data in semi-automated fashion. Furthermore, the tracked horizons must be as reliable as the manually interpreted horizons.

The HorizonCube (Figure 3) is a data element that combines many horizons, typically spaced in the order of the seismic sampling interval (note that the horizon spacing will be laterally varying to reflect thickness changes). A HorizonCube can be created using the strata-slicing methodology. However, the real advantage is in combination with an advanced multihorizon tracking algorithm explained below.

The data-driven multihorizon tracking algorithm is based on following the dip and azimuth of the seismic data. We use dip fields, because they are more continuous than amplitude fields, and less prone to noise. The area in which this is calculated is bounded by at least two framework horizons. Framework horizons are either mapped with a conventional amplitude or dip-steered autotracker. The advantages of the dip-steered tracker are the speed and the tracker's greater awareness of faults. By automatically stopping against mapped fault planes, for example, horizons with watertight intersections at the faults can be generated.

The multihorizon tracking then typically starts at the position of maximum isopach value, and horizons are initiated at seismic sampling density. On 3D sections (or 2D lines), the algorithm extends the horizons outward from the start position. Figure 4 illustrates the workflow. When horizons converge, they continue together; when they diverge, extra horizons will be tracked in a second or later iteration.

When faults are present, the fault throw is calculated by finding the intersection of the fault and the framework horizons. The displacement at the intersections is used to compute the throw at all positions along the fault plane.

The same algorithm can also be applied in a 3D volume. The third dimension, however, adds some more complexity and the need for more intelligent tracking. We solved this problem by tracking the horizons in many circular loops. Each loop results in a realization of a new horizon node z-value. However, when the start and end of the loop do not tie together within a certain threshold, the loop is skipped for further analysis. Statistics are applied to get the best value from the remaining realizations.

Bad data zones can influence the result significantly. It is therefore important to QC the input parameters, and for instance smooth the dip field before applying the algorithm. Another way of circumventing bad data zones is to outline an area where the data quality is high and compute the HorizonCube inside this region only. Alternatively, one can also outline an area where the data quality is particularly low and compute the HorizonCube outside the region. An "editor" can be used to manually correct lower-quality horizons.

Creating a background model

Once the HorizonCube has been established, a background model can be created. This is a straight forward process, where well properties are now interpolated with accurate structural control. In principle, any lateral interpolation algorithm may be used. In our examples, we use inverse distance-based algorithms.

In addition, the HorizonCube can be used to identify sequences (de Bruin et al., 2007). Using this capability, we can find and isolate sequences that have little or no well control because the sequence has been eroded, was not deposited, or is condensed at most or all wells. As interpolating well-log values is not sensible for such sequences, the AI estimates at these sequences without proper well control should be updated manually.

For example, take a sequence not constrained by well data and interpreted as a transgressive sequence. Using the HorizonCube to isolate this sequence in 3D, one can apply an AI trend curve to this sequence that represents a relatively shaly fining-upward depositional trend typical of transgressive sequences.

After interpolation and manual editing, a low-pass fre-

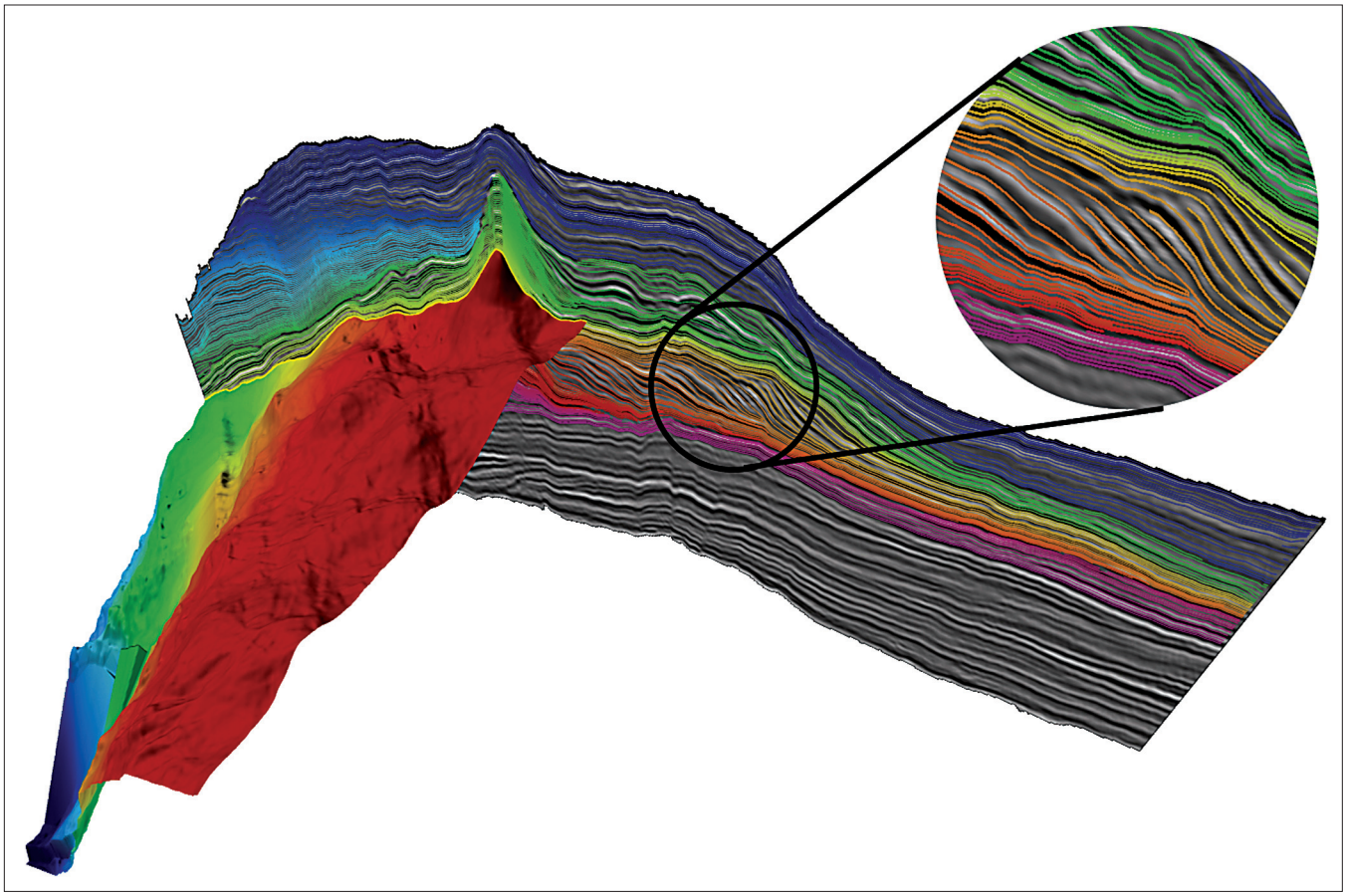

Figure 3. *The HorizonCube is a 3D stack of horizons. In this display, one horizon is displayed in its entirety. Only the intersection of the other horizons with the seismic line is shown. The inset shows the prograding clinoforms, a typical structure best captured with data-driven tracking.*

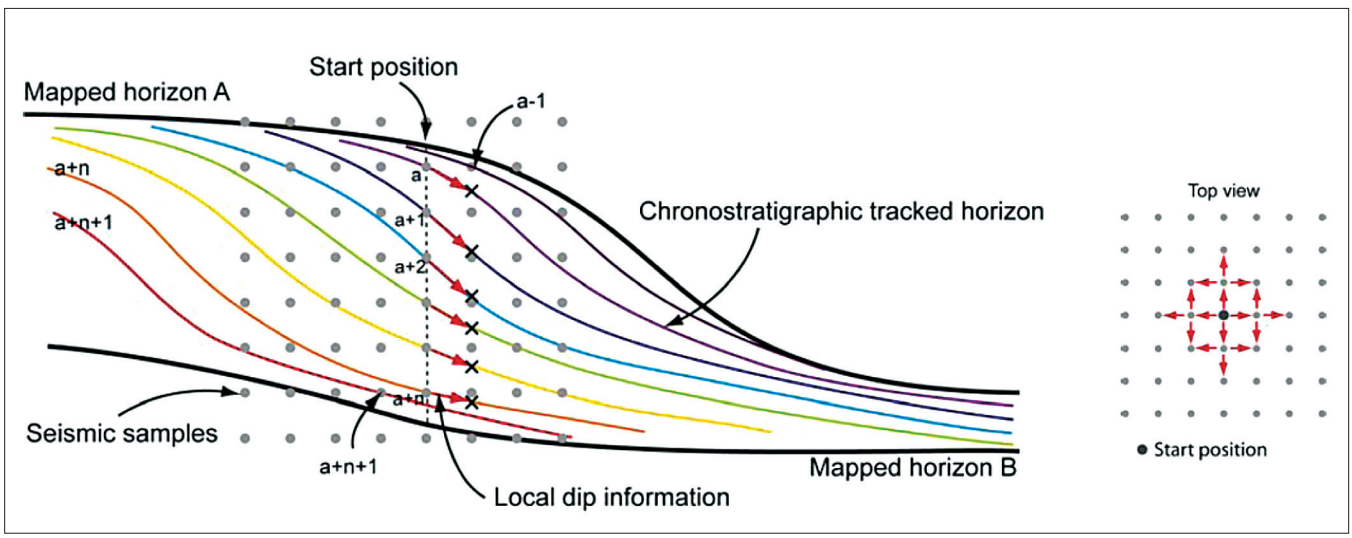

Figure 4. *Principle of data-driven tracking of the HorizonCube using a dip field extracted from the seismic reflectors.*

quency filter is applied to the AI background model. After this filter, the model contains only information about the low-frequency trends not available in the seismic data. After seismic inversion, this low-frequency trend is added to the seismic inversion result in order to arrive at an absolute or broadband seismic inversion result.

The previous workflow is illustrated by two data examples. These examples will illustrate the increased accuracy of the final inversion result using a data-driven HorizonCube. The examples also show that this accuracy is critical for quantitative interpretation of lithology and fluid content from the seismic data. The first example is a North Sea study; the second example is from offshore Brazil.

North Sea acoustic inversion study

The results presented here are largely taken from Huck et

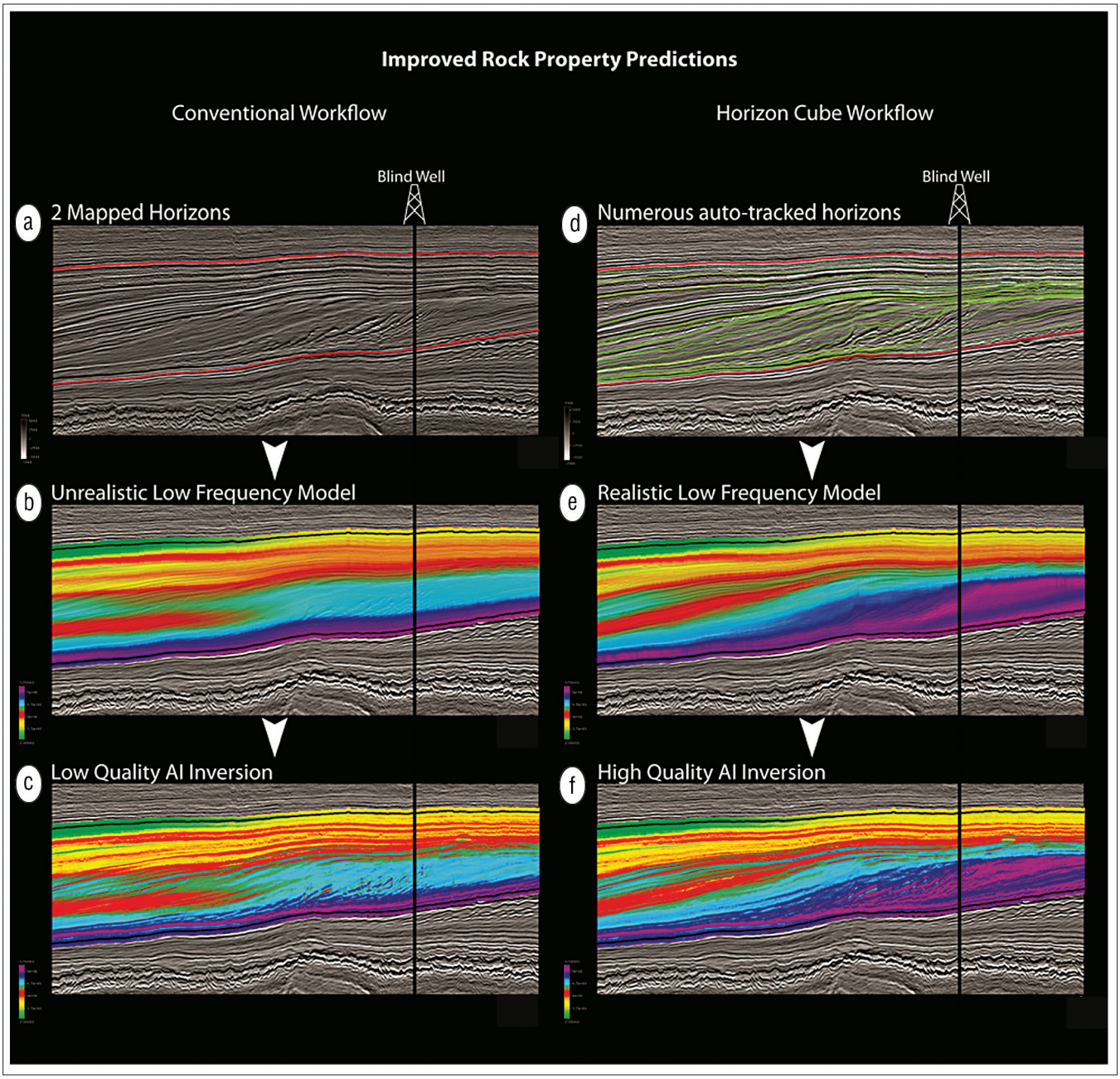

Figure 5. *The difference between (left) conventional workflow and (right) horizon mapping in regard to not only the quality of the model but also the quality of the acoustic impedance (AI) inversion.*

al. (2010) and complemented with an additional sensitivity study. The main reasons to include the results of this earlier study are to (1) demonstrate the repeatability of the results among different seismic data sets and geological environments, and (2) demonstrate the significance of the increase in prediction accuracy, something not done in the original study.

The study is conducted in a clastic deltaic setting, with complex stratigraphic structures, such as coastal wedges, shallow-water to deep-water major clinoforms, and healing phase wedges stacked in a complex fashion.

This study compares two workflows for background model building—the conventional workflow using sparse horizon control, typical for situations with only manual interpreted horizons, and a HorizonCube workflow, using many data-driven horizons for model building The general model on the left of Figure 5 uses only top and bottom horizons to guide the well interpolations. The detailed model on the right uses 19 additional horizons. The simple low-frequency model does not fully honor the seismic while the detailed model does. The inverted results which are driven by the input models reflect these differences.

A blind well was held back from the model building and was used to validate the final results. The graphs in Figure 6, the results of this blind test, show the predicted AI on the vertical axis, and the actual AI in the wells on the horizontal axis. Figure 6a shows the correlation for the inversion with the sparse horizons. Figure 6b shows the correlation for the

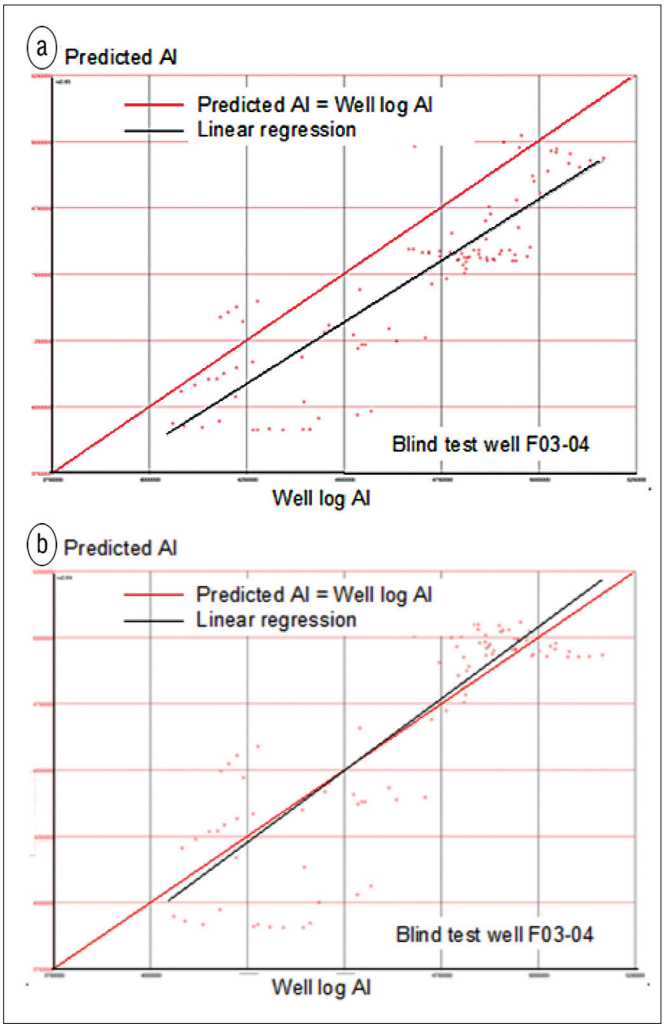

Figure 6. *Crossplots of inverted acoustic impedance versus upscaled well-log (4 ms) acoustic impedance. The red line is the correct answer. The black line is the linear regression through the predicted values. (a) Run 1 (2 horizons) and (b) Run 2 (21 horizons).*

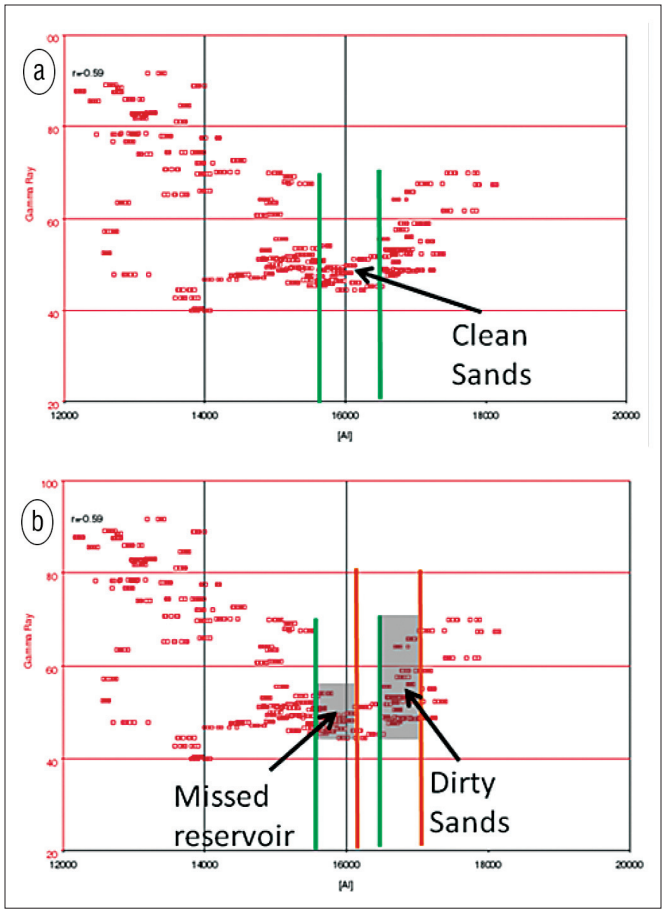

Figure 7. *Illustrating the effect of 4% underprediction in AI. (a) The green bars show the AI limits of the clean sands. (b) The orange bars show which part of the lithology would actually be captured taking into account the underprediction in the inverted AI values. Clean reservoir would be missed and dirty sands would be mapped. AI is in (ft/s) × (g/cm^3).*

HorizonCube-based inversion.

The results show that at this well there is a systematic underprediction of 4% in the AI inversion if the sparse horizon background model is used. The trend is correctly predicted if the HorizonCube-based background model is used. Figure 7 illustrates what 4% underprediction means in terms of lithology prediction. Both graphs in Figure 7 show the same crossplot of GR against AI, with the GR being a good proxy for lithology in this clastic sequence. Figure 7a shows the AI limits between which we can expect our best sands to be located. Figure 7b shows what happens if we take 4% underprediction into account. The important parts of the clean reservoir would be missed, while a significant amount of dirty sand would be selected.

Note that it would not be possible to calibrate this shift and correct for it, as the shifts are not constant over the survey. Where a general background model may lead to underprediction in the inverted AI in one area, it may lead to overprediction of the inverted AI in other areas. The only way to improve the prediction is to improve the background model.

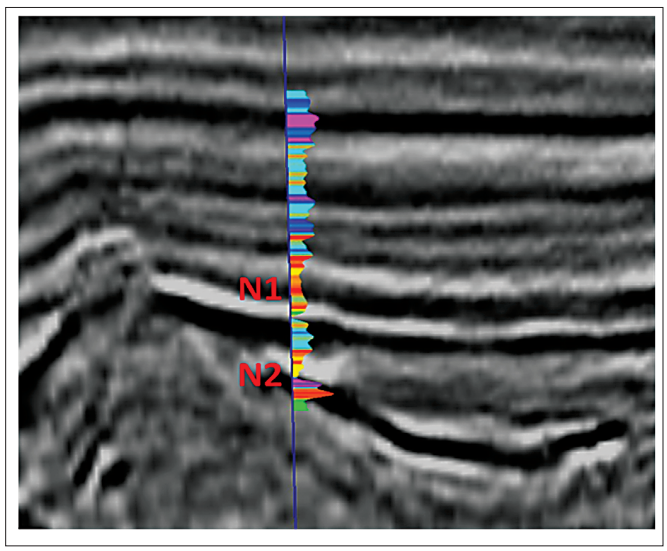

Figure 8. *A seismic section where inversion was applied. The low P-impedance observed from the well log, indicated by N1 and N2, represents the target sandstones under investigation.*

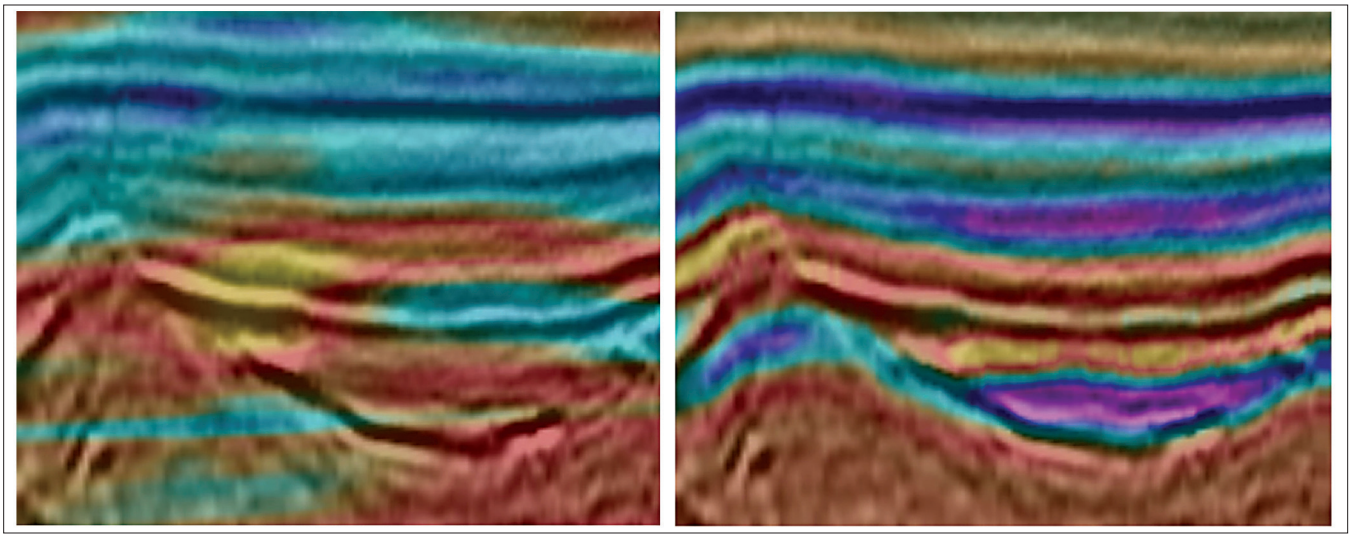

Figure 9. *IP background model before (left) and after (right) HorizonCube, with the latter showing a much better consistency with the geologic structures.*

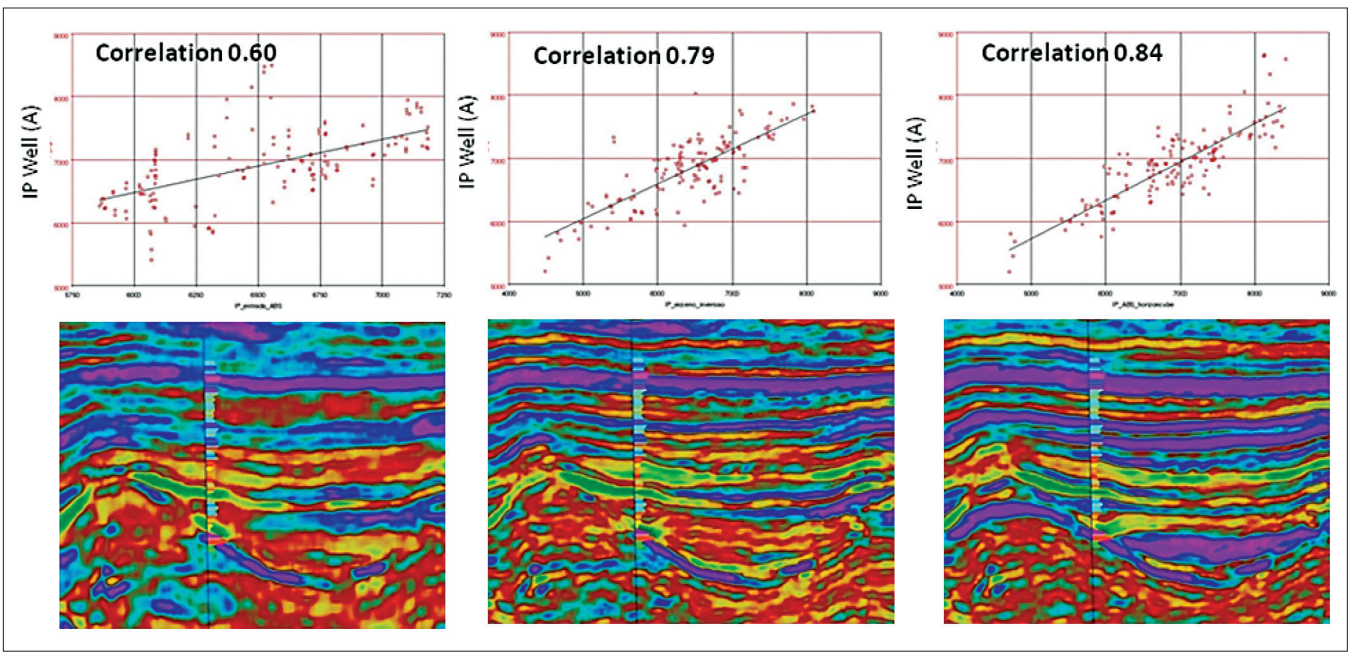

Figure 10. *IP inversion results from the initial inversion to the final result. (left to right) P-impedance obtained from prestack data and original background model; P-impedance from preconditioned data and original background model; and P-impedance with preconditioned data and the HorizonCube-derived background model.*

Field appraisal and reducing development risk offshore Brazil

Another such example of how horizon mapping can improve seismic inversion is the case of Brazilian exploration company OGX which has incorporated horizon mapping into its workflow with the aim of reducing risk in field development. In this particular case, OGX applied high-resolution inversion and horizon mapping to a prospect delineation study in a marine environment offshore Brazil. The main targets were the oil sandstones associated with the low P-impedance values observed in the well log (Figure 8).

A large number of volcanic cones in this area condition the geometry and continuity of sandstone bodies. Prior to this study, one exploration well had been drilled in the area (well A), reaching an oil-filled reservoir. Original amplitude data indicate large lateral continuity of the reservoir layer. The objective here was to delineate the oil-saturated zone of the sand body.

Figure 8 shows the stacked seismic section from the prestack data used as input to elastic inversion. The stacked data were used to derive the HorizonCube. The N1 and N2 reservoirs are the target sandstones under investigation. Rock physics analysis, using P-impedance and S-impedance, showed good separation between the oil-saturated sands and

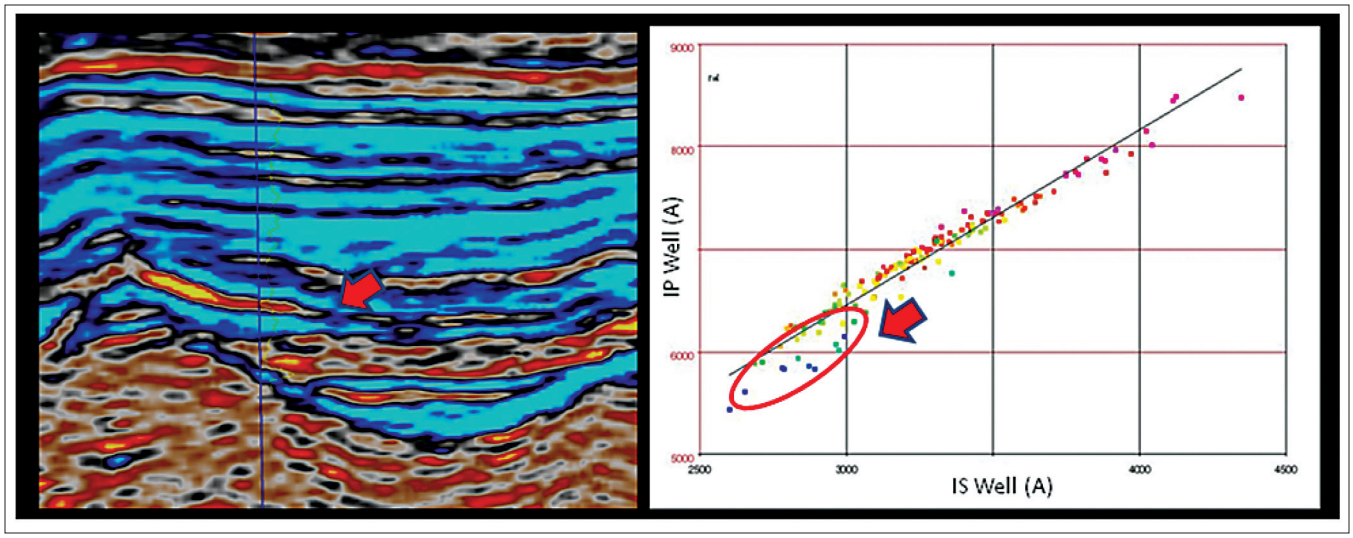

Figure 11. *IP-IS fluid indicator associated with the oil sands indicated in the IP × IS crossplot. The red arrow indicates the possible oil-water contact.*

wet sands, meaning that, with accurate inversion results, we could achieve the desired objective.

The first task was to improve the quality of the seismic information through the preconditioning of the seismic CRP gathers. Secondly, horizon mapping was used to extrapolate the P-impedance and S-impedance logs to create a stratigraphically consistent low-frequency model which incorporates the inversion workflow. Figure 9 compares the previous low-frequency model of P-impedance (left) with the new model (right) which shows greater consistency with the geology.

Comparing the results with the previous inversion, we can clearly see the benefits of incorporating the horizon mapping into the inversion workflow. It should be noted that, with the increased resolution obtained from the inversion, it was possible to correctly map the reservoir thickness and its lateral extension. The improvement of the correlation coefficient between well logs and the inversion results (from the initial inversion to the final deliverable)—provided us with the confidence to proceed in generating fluid indicators.

A volume of IP minus α*IS was derived (where α is a constant calibrated with well data to cancel lithological influence), enabling the illumination of both levels of the reservoir. The improvements of the results can be seen in Figure 10. The arrows in Figure 11 indicate where the fluid indicator dims, suggesting the limits of the oil-saturated sands.

Conclusions

Accurate seismic inversion is a key tool for risk reduction, as it can extract changes in the elastic properties of the subsurface due to lithology and fluid variations. However, as changes may be subtle, errors due to generalized background models may lead to significant error in lithology or fluid prediction. Areas with complex structuring either of stratigraphic or tectonic origin are prone to model errors if standard model-building workflows are used.

However, from the results obtained with high-resolution inversion and the incorporation of a stratigraphically consistent low-frequency model generated through increased automatic horizon mapping, it was possible to greatly improve the quality of the estimation of the subsurface parameters in structural complex settings. We showed that the data-driven workflow is repeatable and robust within two different seismic data and geological settings. TLE

References

De Bruin, G., N. Hemstra, and A. Pouwel, 2007, Stratigraphic surfaces in the depositional and chronostratigraphic (Wheeler transformed) domain: The Leading Edge, **26**, 883–886.

Huck, A., G. Quiquerez, and P. de Groot, 2010, Improving seismic inversion through detailed low-frequency model building: 72nd EAGE Conference & Exhibition.

Russell, B. and D. Hampson, 1991, A comparison of poststack seismic inversion methods: 61st Annual International Meeting, SEG, Expanded Abstracts, 876–878.

Zeng H., M. M. Backus, K. T. Barrow, and N. Tyler, 1998a, Stratal slicing, part I: Realistic 3-D seismic model: Geophysics, **63**, no. 2, 502–513.

Zeng H., S. C. Henry, and J. P. Riola, 1998b, Stratal slicing, part II: real seismic data: Geophysics, **63**, no. 2, 514–522.

Acknowledgments: We thank OGX for permission to publish these results, especially Marcos do Amaral for his innovative thinking and his willingness to always incorporate leading-edge technologies to solve exploration challenges.

Corresponding author: friso.brouwer@dgbes.com